

Noise figure of PbSe-quantum dot fiber hybrid Raman amplifier

O. MAHRAN^a, N. EL-NOHY^a, H. IBRAHIM^{a,b,*}

^aFaculty of Science, Physics Department, Alexandria University, Mohrambeik 21511, Alexandria, Egypt

^bFaculty of Engineering, Basic Engineering Science Department, International Academy of Engineering and Media Science, Cairo, Egypt

Noise figure (NF) of the simulation of a hybrid multi-doped PbSe Quantum Dot (QD)/Multi-pumped Raman fiber amplifier for several commercial Raman fibers, which would present a highly tunable optical amplifier are presented. The NF dependence on the Raman fiber length and pumping power, the PbSe QD fiber length, and pumping power are studied and analyzed. Our results are presented graphically and show an increase in the NF with increasing the Raman fiber length and pumping power, however, the NF decreases at higher wavelengths with increasing PbSe QD fiber length and pumping power. Curves for different Raman lengths all converge to a value around 3.3 dB with increasing signal wavelength, this is also observed for different Raman fiber lengths curves. A QD fiber of length 20 cm with 300 mW pumping power decreases the NF of the Raman only fiber by around 6.0 dB, the same decrease in NF is also observed by a 150 mW pumped QD fiber with a 44 cm length.

(Received October 8, 2020; accepted June 11, 2021)

Keywords: Raman, Quantum dots, Hybrid optical amplifier, Noise Figure

1. Introduction

Optical amplifiers play an important role in Dense Wave Division Multiplexing (DWDM). Thus, several optical amplifiers have been proposed ranging from Raman type to rare-earth and more recently quantum dot (QD) amplifiers optical amplifiers. The effect of an optical amplifier on the noise to signal ratio is an important characteristic for any proposed amplifier and is usually measured through the noise figure (NF). Beshr et al. [1] introduced a new model for the NF of Distributed Raman Amplifiers (DRA) and studied their behavior for different pumping schemes and found that the noise figure (NF) increases exponentially with the fiber length and decreases exponentially with the signal input power. Iqbal et al. [2] reported a dual-stage broadband discrete Raman amplifier that improved the low wavelength by 3.3 dB. Almukhtar et al. [3] demonstrated a wideband erbium-zirconia-yttria-aluminum co-doped fiber with a noise figure that is maintained below 10 dB within a 17.1 dB flat gain region. Kumar et al. [4] investigated a Raman-Thulium-doped Tellurites fiber hybrid optical amplifier with an NF less than 5 dB while Kaur et al. [5] studied a Semiconducting Optical Amplifiers (SOA)/Erbium Doped Amplifier (EDFA)/Raman hybrid amplifiers and obtained a noise figure of less than 5.7 dB. They also investigated the effect of the pumping power distribution on the gain, noise figure, and gain flatness of this hybrid amplifier [6]. Mahran [7] studied the gain and noise enhancement of a Hybrid $\text{Er}^{+3}/\text{Yb}^{+3}$ co-doped fiber/Raman hybrid amplifier and the effect of micro and macro-bending on the gain and noise of a hybrid EDFA/Raman amplifier has been studied by Mahran [8]. Interest in the use of quantum dots as

optical amplifiers has increased over the years where Cheng et al. [9] studied through numerical simulation the characteristics of a PbSe-QD optical amplifier. Cheng et al. [10] also studied the gain and noise characteristic of a multi-doped PbSe. More recently experimental realization of a PbSe-QD ultrawideband by Cheng et al. [11]. An experimental realization of a PbSe-QD doped amplifier based on sodium-aluminum-borosilicate-silicate was achieved by Cheng et al. [12] where the bandwidth and noise were found to be superior to EDFA amplifiers. Focus on the study of hybrid amplifiers has been on EDFA or EDFA related fibers/Raman fibers amplifiers, where the gain and noise characteristics are restricted by the intrinsic properties of the photoluminescence and absorption properties of Erbium ions. In this report, we study the noise characteristic behavior of a proposed PbSe-QD fiber/Raman fiber amplifier by changing the size and distribution of the QDs, the pumping scheme and pumping wavelengths of the Raman fiber. This proposed hybrid amplifier would have the advantage of having highly tunable properties [13], [14]. This study is done through numerical simulation where we study the variation of the NF of the proposed amplifier by varying the Raman fiber length and pumping power and also PbSe-QD fiber length and pumping power. In this report, we give a description of the theory and equations of the model used to simulate our proposed hybrid amplifier in section 2. Our results are then presented graphically and discussed in section 3. Finally, our concluding remarks are given in section 4.

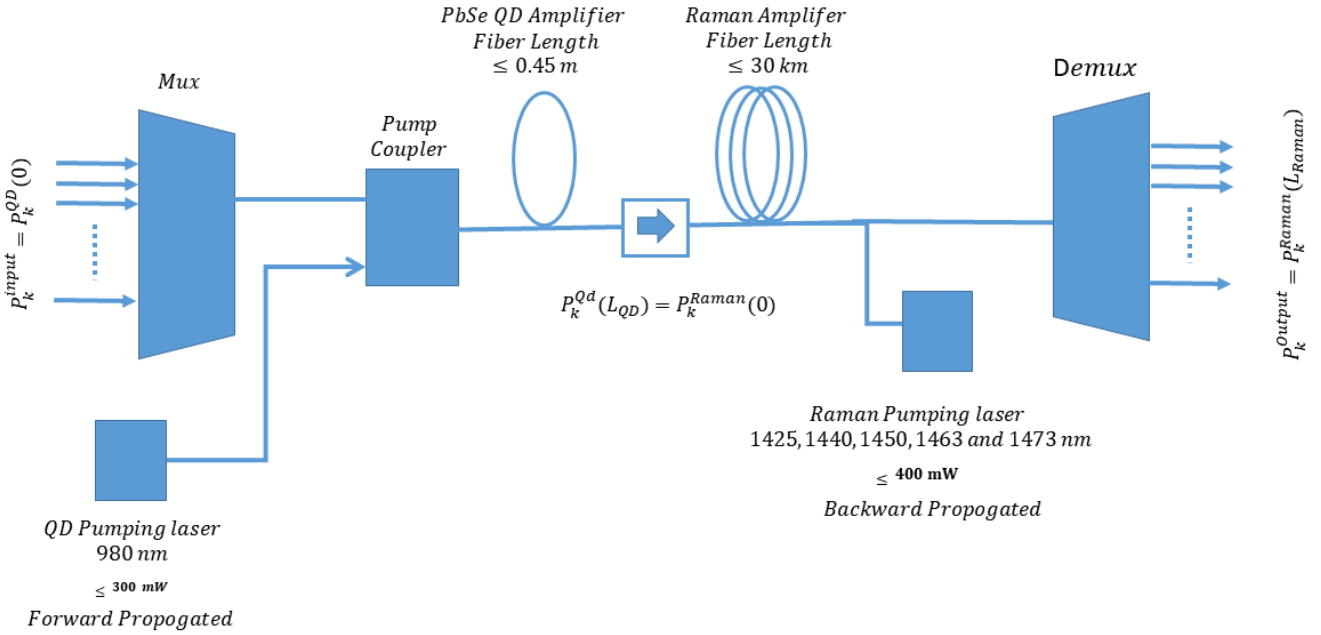


Fig. 1. The schematics of the proposed PbSe-QD/Raman amplifier

2. Theory and modeling

A schematic for the hybrid multi-doped PbSe-QD/Raman amplifier is shown in Fig. 1 where multi-doping is assumed as a multi-quantum-dot doping of three different diameters of $5.5 \text{ nm} \pm 10\%$ as in Cheng et al. [10]. The output power from the PbSe-QD amplifier from the signal/noise $P_k^{QD}(L_{QD})$ channel k is used as the input power for the Raman amplifier $P_k^{Raman}(0)$ and L_{QD} is the length of the PbSe-QD fiber. The input signal/noise for the k channel P_k^{input} is used as the input power for the signal/noise power for PbSe-QD amplifier and the output signal for channel k is the same as the output of the Raman amplifier. It is also important to mention that for the PbSe-QD only amplifier, the input signal power goes through the first PbSe-QD fiber only, and its output $P_k^{QD}(L_{QD})$ is used to calculate the NF for the PbSe only amplifier as described in subsection 2.1. The same happens for the Raman only amplifier, where the input signal propagates directly through the Raman only fiber on the second stage of the above schematic and its output is used to calculate the NF as described in subsection 2.2.

2.1. Quantum Dot Amplifier

The PbSe Quantum Dot fiber electronic spectrum is attributed to $1P_e - 1P_h$, $1S_{e(h)} - 1P_{h(e)}$ and $1S_e - 1S_h$ electronic transitions in a wavelength range that starts from 800 nm to around 1800 nm as shown in Fig. 2. The absorption and emission cross-sections for a 5.5 nm diameter were measured by Cheng et al [10] as shown in Fig. 3, it is well known that the emission cross-section

peak wavelength could be determined from the Beer-Lambert law Eq. 1

$$A = \epsilon CL \quad (1)$$

and the following phenomenological Eq. (2)

$$\epsilon = 1600 \Delta E (D)^3 \quad (2)$$

where A is the molar absorbance, ϵ is the molar attenuation coefficient, C is the molar concentration, L is the length of the radiation path, D is the QD diameter and ΔE is the first emission photon energy. By changing the radius of the QD, the signal wavelength range over which amplification is desired can be changed. In this report, the PbSe-QD amplifier is modeled as a three-level system where the rate equations for the model are given by Eq. (3), Eq. (4), and Eq. (5), and the radiation power along the PbSe QD fiber is given by Eq. (6) [9], [10], [15], [16], where n_1, n_2 and n_3 are the population numbers for the ground state, the second level and the third level respectively, $P_k(z)$ is the radiation power for the signal, amplified spontaneous emission (ASE) noise, or the pump channel k . σ_{ak} and σ_{ek} are the absorption and emission cross-section, $i_k(r)$ is the radial radiation profile, A_{21} and A_{32} are the spontaneous decay probability per unit time for the $2 \rightarrow 1$ and $3 \rightarrow 2$ transitions. The PbSe-QD fiber amplifier is a forward pumped at a wavelength of 980 nm and default pumping power of 300 mW, ν_k is a bandwidth equal to $\Delta\nu_k$, l_k represents the scattering attenuation cross-section, i_k represents the transversal modal intensity, a represents the core radius. In Eq. (6), the first and second terms represent the stimulated emission due to the

signal/pump powers and the noise respectively. Here $m=2$ for the signal and ASE equations and $m=0$ for the pump power. The third term represents the absorption rate and the second term represents the attenuation due to scattering. We use the stationary state approximation where $\frac{dn_1}{dt} = 0$ and $\frac{dn_2}{dt} = 0$ are used in Eq. (3) and Eq. (4). The n_1, n_2 and n_3 are solved in terms of P_k and are substituted in Eq. 5 and then solved along the fiber from $P_k(z)$ along the fiber. The parameters used in the simulation of the PbSe-QD fiber can be found in Table 1.

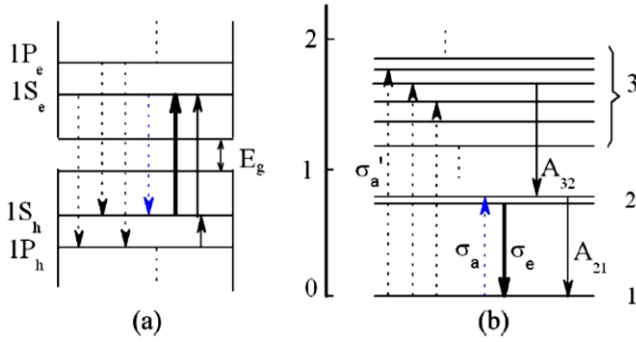


Fig. 2. Schematic diagram of the electronic transitions for the PbSe-QD [12],[10]

2.2. Raman amplifiers

The radiation power equations propagation along the Raman amplifier are given by Eq. (7), Eq. (8), and Eq. (9) [17]. The \pm symbol denotes the forward and backward propagated powers respectively. For Eq. (6), the first term represents the attenuation decay and the second term represents Rayleigh backward scattering, the third and fourth represent the power and ASE gain, and finally, the fifth term represents the depletion in power due to stoke conversion. A description of the parameters in Eq. (7) is given in Table 2 and the Raman gain is calculated from the Raman gain efficiency C_r as shown in Eq. 8. For the commercial fibers under consideration, we use a normalized gain efficiency $C_{normalized}$ multiplied by a peak value C_{peak} that is dependent on the commercial Raman fiber as shown in Eq. (8). The normalized gain efficiency used in the simulation is shown in Fig. 4. The values of C_{peak} for different commercial Raman fibers are shown in Table 2. In this report, the output power from the QD amplifier is used as the input for the backward-pumped Raman fiber $P_k^{Raman}(0)$. Eq. (6) is then integrated along the Raman fiber of length L to calculate its radiation power output $P_k^{Raman}(L)$ which is assumed to be the output of the hybrid fiber for the signal channel k – which is either a signal or an ASE noise channel.

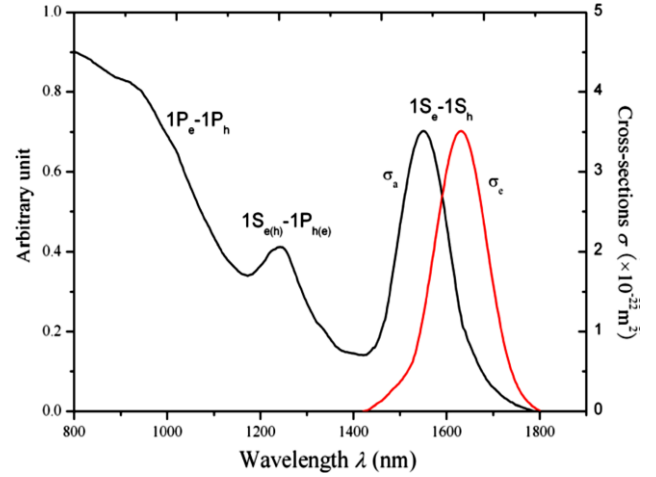


Fig. 3. The absorption and emission cross-section of 5.5 nm diameter PbSe-QD [9] (color online)

$$\frac{dn_1}{dt} = -\sum_k \frac{P_k(z) i_k(r) \sigma_{ka}}{h\nu_k} n_1(r, z) + \sum_k \frac{P_k(z) i_k(r) \sigma_{ke}}{h\nu_k} n_2(r, z) + \frac{P_p(z) i_p(r) \sigma_{ep}}{h\nu_p} n_3(r, z) \quad (3)$$

$$\frac{dn_2}{dt} = \sum_k \frac{P_k(z) i_k(r) \sigma_{ka}}{h\nu_k} n_1(r, z) - \sum_k \frac{P_k(z) i_k(r) \sigma_{ke}}{h\nu_k} n_2(r, z) - A_{21} n_2(r, z) + A_{32} n_3(r, z) \quad (4)$$

$$n_3 = n - n_2 - n_1 \quad (5)$$

The Raman fiber is backward pumped at wavelengths at 1425 nm, 1440 nm, 1450 nm, 1465 nm, and 1473 nm at a default value of the pumping power of 400 mW. The NF is defined as the signal to noise ratio at the output (SNR_o) to the signal to noise ratio at the input (SNR_i) as shown in Eq. (10) [7], [10]. For the NF calculation, we use Eq. (11) and Eq. (12) [10], where $G_s(\lambda)$ is the gain at wavelength λ , while $P_{ASE}(\lambda)$ is the ASE noise power at this wavelength.

3. Results and discussion

Here, we present NF of the proposed PbSe-QD/Raman amplifier simulation and its dependence on the parameters of the constituent amplifier. Unless explicitly stated to be otherwise, the default values for the simulation parameters are 44 cm for the PbSe-QD fiber length, 300 mW for the PbSe-QD pumping power, 30 km for the length of the Raman fiber, and a Raman pumping power of 400 mW.

$$\frac{dP_k(z)}{dz} = u_k \sigma_{ek} \int_0^a i_k(r) n_2(r) [P_k(z) + mh\nu_k \Delta\nu_k] 2\pi r dr - u_k \sigma_{ek} \int_0^a i_k(r) n_2(r) [P_k(z)] 2\pi r dr - l_k P(z) \quad (6)$$

$$\begin{aligned} \frac{dP_v^\pm}{dz} &= \mp \alpha_v P_v^\pm \pm \epsilon_v P_v^\mp \pm P_v^\pm \sum_{\mu > \nu} \frac{g_{\mu\nu}}{\Gamma_{Aeff}} (P_\mu^+ + P_\mu^-) \pm \\ &2\hbar\nu\Delta\nu \sum_{\mu > \nu} \frac{g_{\mu\nu}}{\Gamma_{Aeff}} (P_\mu^+ + P_\mu^-) (1 + \eta(T)) \mp \\ &P_v^\pm \sum_{\mu < \nu} \frac{\omega_\nu}{\omega_\mu} \frac{g_{\mu\nu}}{\Gamma_{Aeff}} (P_\mu^+ + P_\mu^-) \pm \\ &4\hbar\nu\Delta\nu \sum_{\mu < \nu} \frac{\omega_\nu}{\omega_\mu} \frac{g_{\mu\nu}}{\Gamma_{Aeff}} (P_\mu^+ + P_\mu^-) (1 + \eta(T)) \end{aligned} \quad (7)$$

$$C_r(\mu - \nu) = \frac{g_{\mu\nu}(\mu - \nu)}{\Gamma_{Aeff}} \quad (8)$$

Table 1. PbSe-QD Amplifier Parameters

Parameter	Symbol	Value
Core radius	a	4.1×10^{-6} m
Concentration of QD particles for each radius	N	1.0×10^{21} m ⁻³
Scattering attenuation coefficient	l_k	0.03 dB/m
Propagation direction sign	u_k	Forward +, Backward -
Pumping power input	$P_p(0)$	Up to 300 mW
Pumping power Wavelength	λ_p	980 nm
Signal power input	$P_p(0)$	1.0×10^{-5} W
Channel Bandwidth	$\Delta\lambda_p$	1 nm
Number of channels	N_{ch}	101
Minimum wavelength for the channel	λ	1525 nm

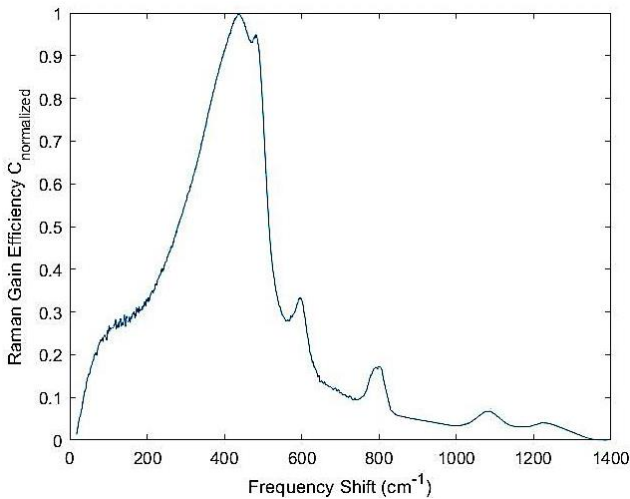


Fig. 4. Normalized Raman gain efficiency

$$C_r = C_{peak} C_{normalized} \quad (9)$$

$$NF(\lambda) = \frac{SNR_o}{SNR_i} \quad (10)$$

$$NF(\lambda) = \frac{2n_{sp}(\lambda)[G_s(\lambda)-1]+1}{G_s(\lambda)} \quad (11)$$

$$n_{sp} = \frac{P_{ASE}(\lambda)}{\hbar\nu_k\Delta\nu[G_s(\lambda)-1]} \quad (12)$$

Table 2. Raman Amplifier Parameters

Parameter	Symbol	Value
Absorption Coefficient	α_k	0.18 – 0.28 dB/km
Raman Gain Efficiency	C_p	Allwave=0.36 W ⁻¹ km ⁻¹
		SMF=0.39 W ⁻¹ km ⁻¹
		CorningNZ-DSf=0.72 W ⁻¹ km ⁻¹
		CorningDSF = 0.67 W ⁻¹ km ⁻¹
Rayleigh Backscattering	ϵ_k	TrueWave RS = 0.6 W ⁻¹ km ⁻¹
		LEAF=0.46 W ⁻¹ km ⁻¹
Pumping wavelengths	$\lambda_{p1}, \lambda_{p2}, \lambda_{p3}, \lambda_{p4}, \lambda_p$	1425,1440,1450,1465 1473 nm
Channel Bandwidth	$\Delta\nu = \frac{c\Delta\lambda}{\bar{\lambda}}$	1 nm
Number of channels	N_{ch}	100
Minimum wavelength for the channel	λ_{min}	1525 nm

Fig. 5 shows the dependence of the noise figure on the variation of the Raman fiber length for several commercial fibers. The remaining parameters – Raman fiber pumping powers, PbSe QD fiber length, and pumping power are assumed to be of the default values. It is also observed that for all signal wavelengths and all Raman fibers, the NF decreases with increasing signal wavelengths. This is due to the effect of the SRS gain efficiency that increases with increasing wavelength and the amplification of the signal as it propagates through the Raman fiber signal which in turn reduces the NF through signal amplification. The NF also increases generally with increasing Raman fiber length due to ASE and attenuation by increasing absorption, however, the rate of increase of the NF is lowered with higher values of wavelength. The NF ranges also depend on the type of commercial Raman fiber and

the Raman fiber length. The curves then converge to a minimum that is around 3.2 dB, and this minimum is almost independent of the Raman fiber type. The factors that mostly affect the NF are the amplification of the signal by the stimulated Raman scattering (SRS) which lowers the NF with increasing Raman fiber length, the ASE process and signal attenuation across the fiber - the

latter two increase the NF with increasing Raman fiber length. For longer wavelengths, the decrease of the NF by SRS amplification compensates the increase of the NF by ASE and signal attenuation, while for shorter wavelength, the SRS cross-section is lower, thus the latter two processes dominate and the NF increases with increasing Raman fiber length.

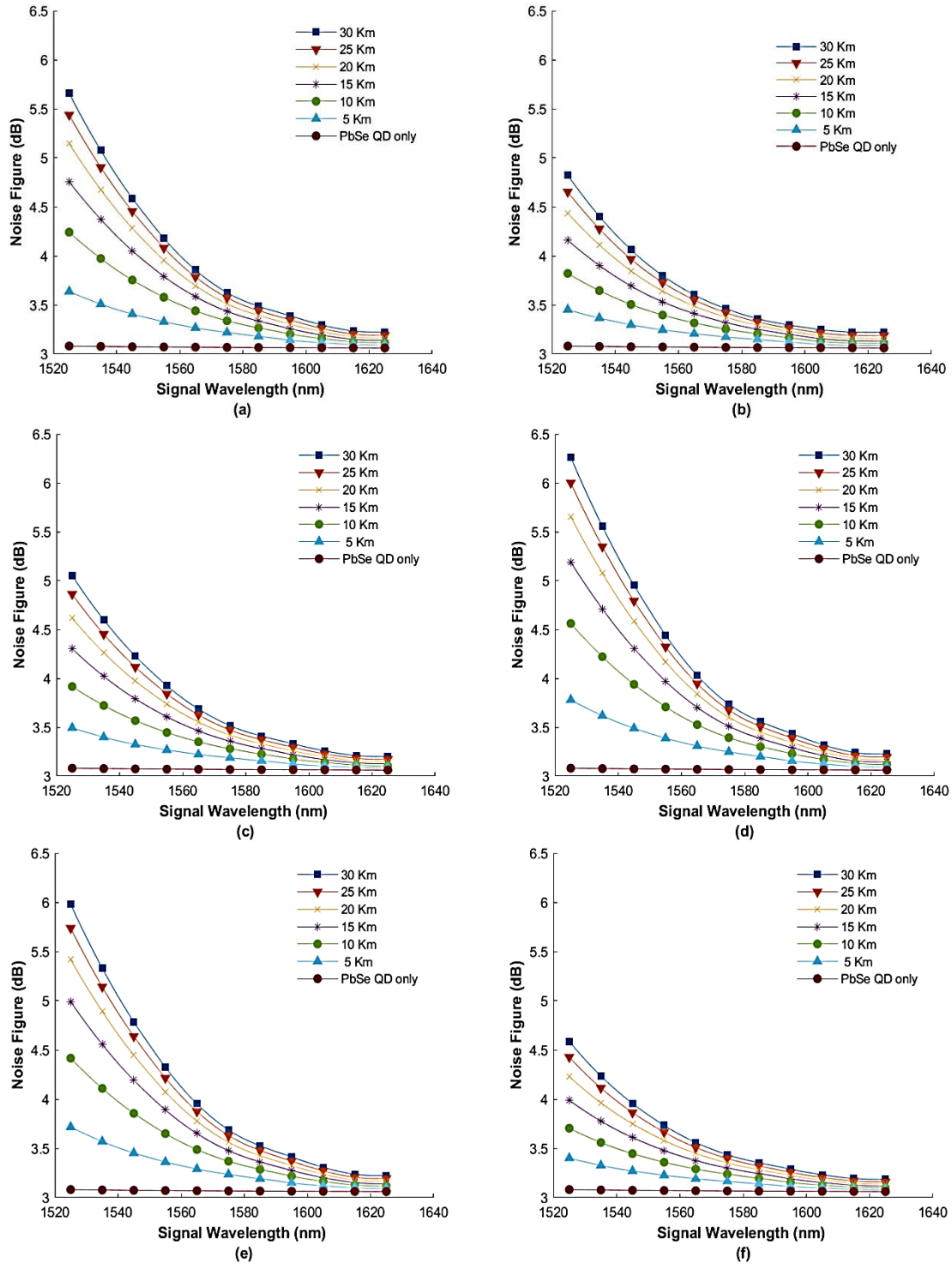


Fig. 5. Hybrid Amplifier NF dependence on Raman fiber length for (a) TrueWave Raman fiber (b) SMF Raman fiber (c) LEAF Raman fiber and (d) Corning NZDSF Raman fiber (e) Corning DSF Raman fiber and (f) AllWave Raman fiber (color online)

Fig. 6 shows the dependence of the NF on the Raman pumping power for various commercial Raman fibers. The variation is similar to the behavior of the NF with the variation of the Raman fiber length where again the hybrid amplifier NF increases with increasing Raman pumping power which is due to the increase of ASE with higher pumping power as it propagates through the fiber. The rate of increase itself is reduced with the rise of the input signal

wavelength, thus the NF decreases from a maximum value that is also dependent on the type of the Raman fiber and the Raman pumping power. Moreover, the curves converge to a minimum of 3.3 dB, which is independent of the Raman pumping power and type, this again can be explained by SRS signal amplification that lowering the NF and the SRS gain efficiency being higher for longer wavelengths.

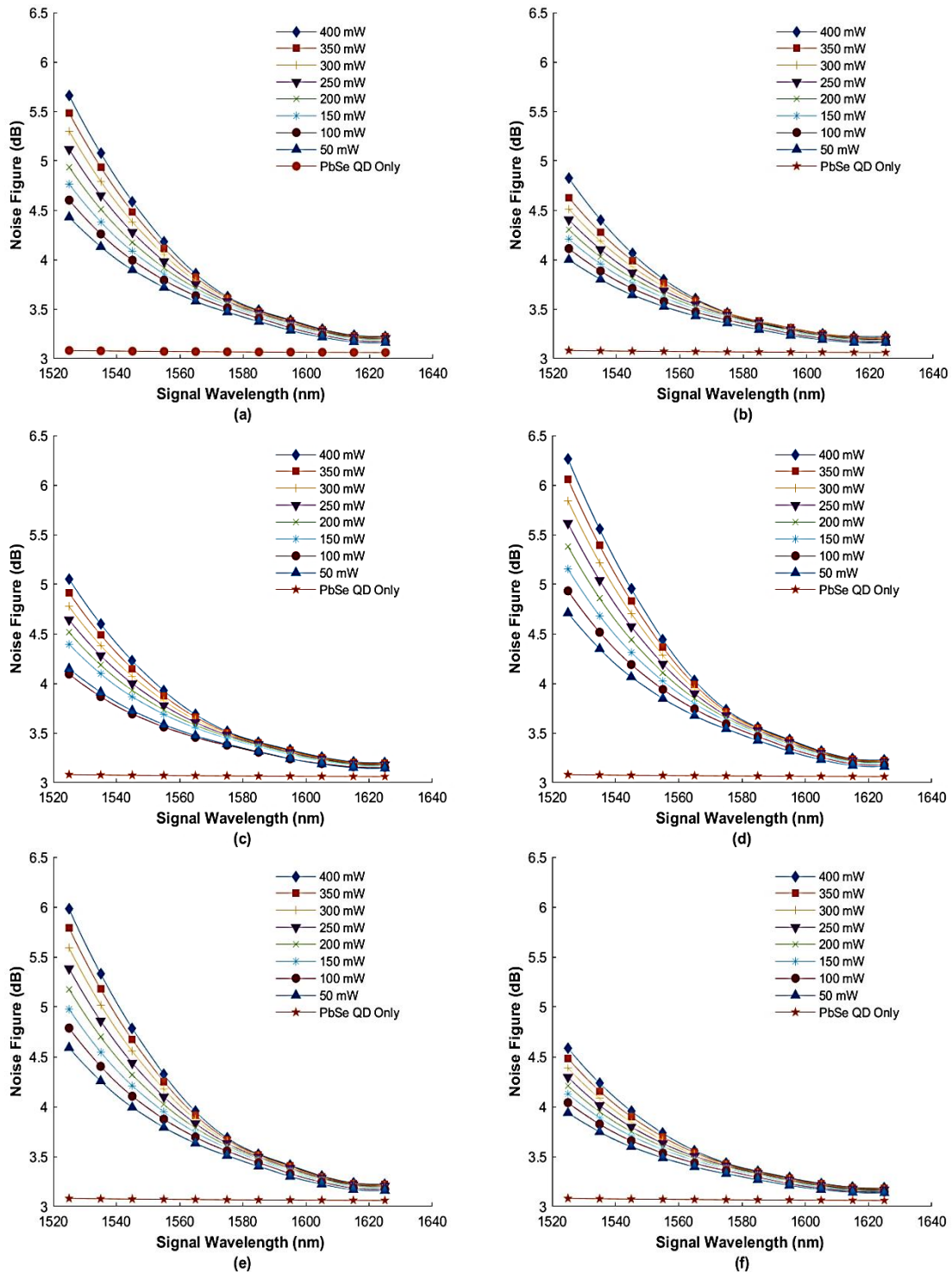


Fig. 6. Hybrid Amplifier NF dependence on Raman pumping power for (a) TrueWave Raman fiber (b) SMF Raman fiber (c) LEAF Raman fiber and (d) Corning NZDSF Raman fiber (e) Corning DSF fiber and (f) AllWave Raman fiber (color online)

Fig. 7 shows the dependence of the hybrid PbSe QD/Raman fiber NF on the PbSe-QD fiber length for the Raman commercial fibers under consideration. The behavior is a little more complicated because there are different trends seen at lower and higher wavelengths. It is interesting to see that for the PbSe-QD fibers longer than 20 cm, the NF for the different lengths of QD fiber intersects at certain wavelengths that also depend on the type of Raman fiber. It is around 1565 nm for almost all fibers except for Corning DSF and Corning NZDSF which is around 1585 nm. These interceptions define the boundary of lower and higher wavelengths in this discussion. In general, the use of a hybrid amplifier at lower wavelengths decreases the NF to a minimum as the length of the PbSe-QD fiber increases up to 30 cm, however at this length and beyond, the NF changes to

increase with increasing fiber length. It seems that the increase in NF with longer QD fiber is due to QD and Raman fibers ASE, in which the signal attenuation is exactly compensated by stimulated emission amplification (SEA) inside both fibers. At longer wavelengths above the intercept, the NF decreasing with increasing PbSe-QD fiber length and the value becomes constant about 3.5 dB at greater or equal to 40 cm. However, the NF could be considered almost constant after 20 cm (<1.0 dB) due to the observation that 30 cm is enough to absorb almost all of the 300 mW pumping power, and an increase of the fiber length leads to only a slight attenuation which is small owing to the QD fiber being only a couple of centimeters long. It is also shown that the optimum PbSe-QD fiber length of 40 cm for all types of Raman fiber.

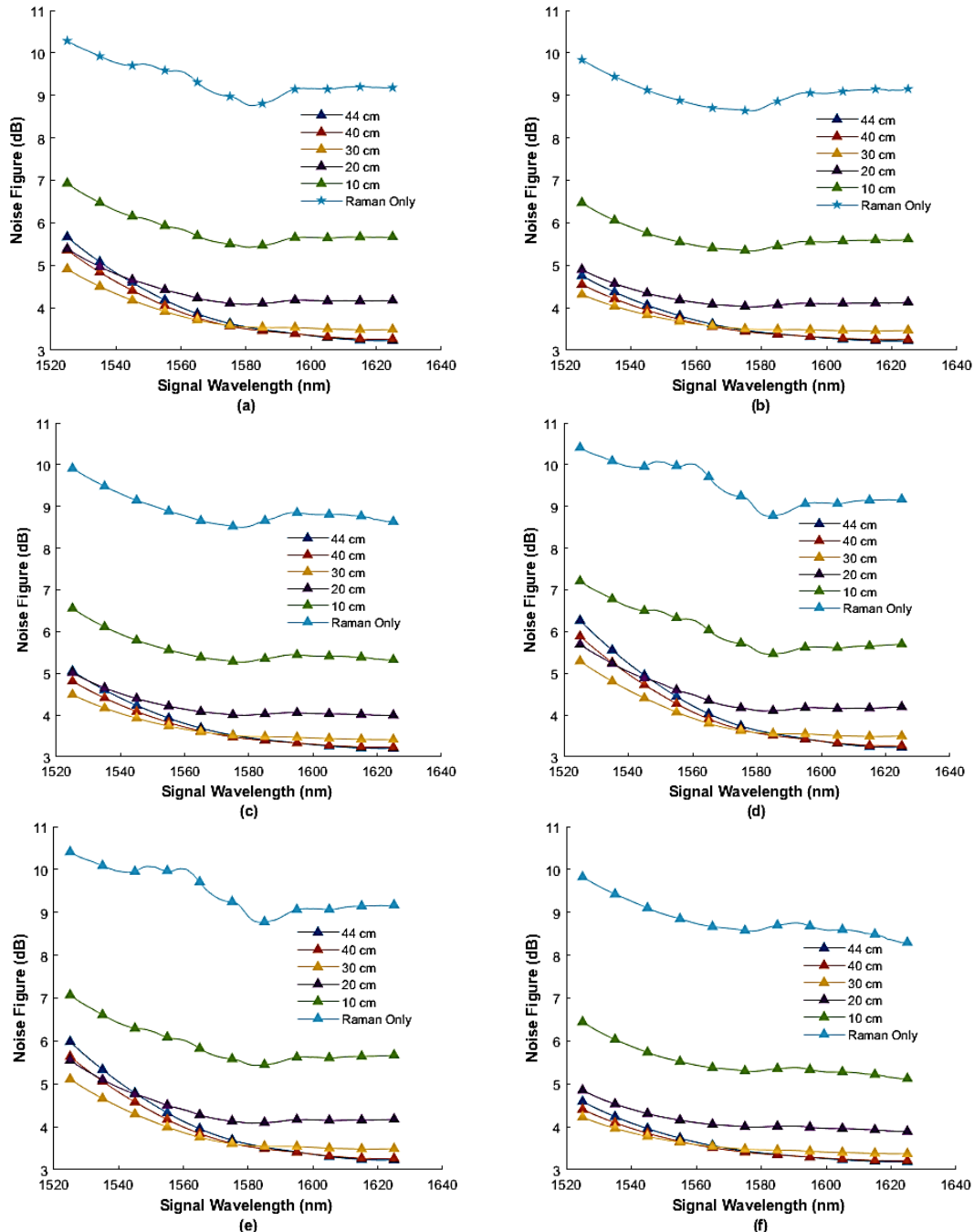


Fig. 7. Hybrid Amplifier NF dependence on PbSe-QD fiber length for (a) TrueWave Raman fiber (b) SMF Raman fiber (c) LEAF Raman fiber and (d) Corning NZDSF Raman fiber (e) Corning DSF fiber and (f) AllWave Raman fiber (color online)

Fig. 8 shows the dependence of hybrid PbSe QD fiber/ Raman fiber NF on the PbSe-QD pumping power for all commercial fibers under study. We see that for PbSe-QD fiber pumping power greater than 100 mW, the hybrid PbSe-QD/Raman amplifier NF is almost independent of the PbSe-QD pumping power. Since a slight increase of < 1 dB is observed, thus the NF is seemed to be independent of the PbSe QD pumping power as there is only a slight change that is less than 1 dB with increasing pumping power from 50 to 300 mW. The use of the PbSe-QD amplifier decreases the NF of the Raman only amplifier by as much as 6 dB. Furthermore, the trend of the NF remains almost constant after 100 mW PbSe-QD

pumping power which is due to the signal amplification by Stimulated Emission that seems to reach a saturation value at 150 mW. It is also interesting to observe that the NF curves for all variation of PbSe-QD fiber pumping powers intersect at certain wavelengths that depend on the type of Raman fiber. And it seems that at lower wavelengths, the effect of increasing the PbSe pumping power has resulted a slight increase in the ASE and increase the value of the NF slightly. However, at higher wavelengths beyond the intersection, the increase in pumping power compensates the effect of SRS signal amplification, thus reduces the NF.

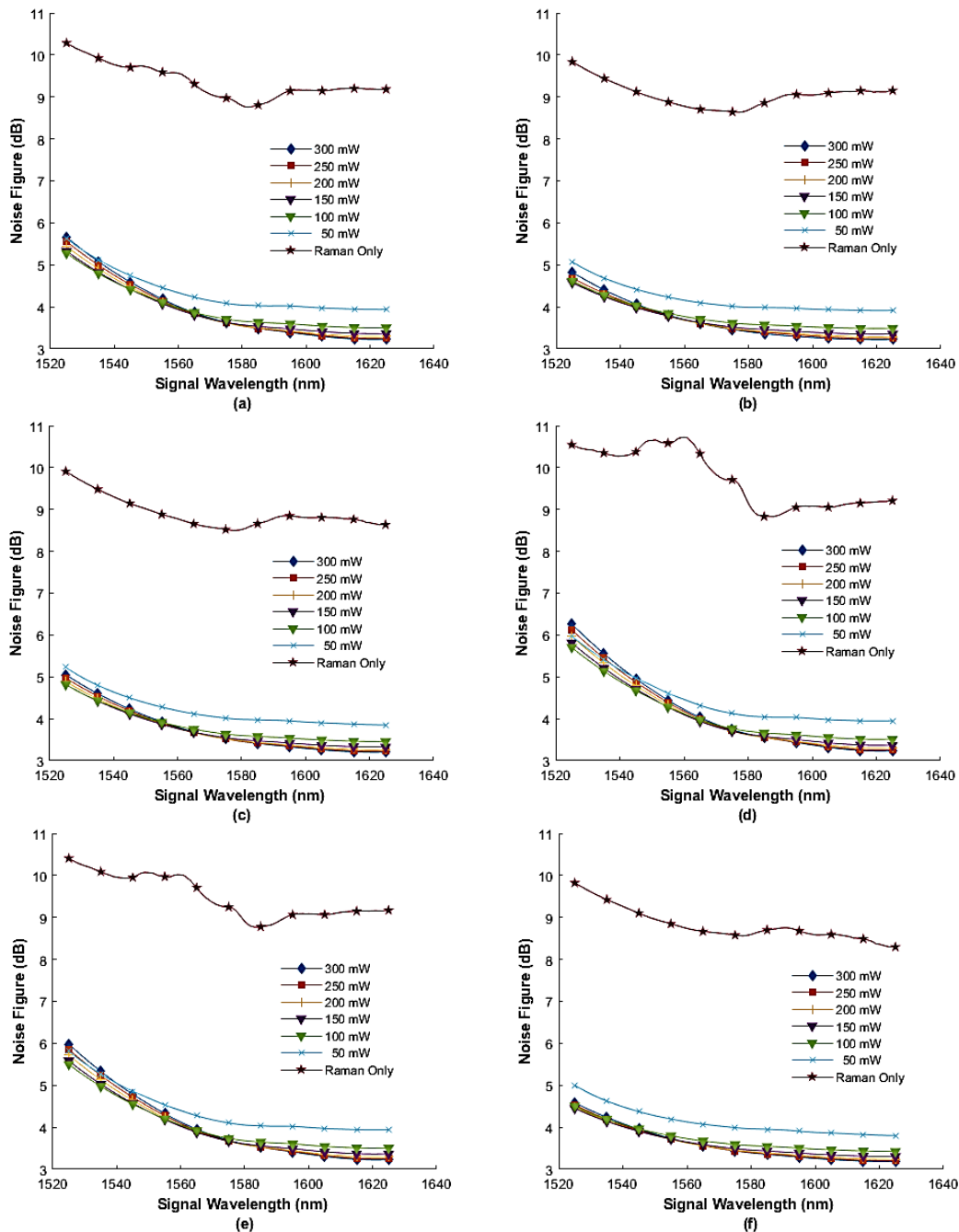


Fig. 8. Hybrid Amplifier NF dependence on PbSe-QD pumping power for (a) TrueWave Raman fiber (b) SMF Raman fiber (c) LEAF Raman fiber and (d) Corning NZDSF Raman fiber (e) Corning DSF fiber and (f) AllWave Raman fiber (color online)

Table 3 shows the maximum NF values for the proposed hybrid PbSe-QD/Raman amplifier at the default PbSe fiber length of 44 cm and pumping power of 300 mW, and the Raman pumping power of length 30 km and the maximum pumping power of 400 mW. The values are compared to the same values for Raman only and PbSe-QD only amplifiers with the same lengths and pumping powers. Table 4 shows the maximum NF obtained for PbSe-QD/Raman amplifier using default values of fiber lengths and pumping powers of the PbSe-QD and Corning DSF Raman fiber, compared to EDFA and EDFA/Raman amplifiers as given by Mahran et al. [18].

Table 3. Maximum NF for Hybrid, Raman only, and PbSe-QD amplifiers for each type of Raman fiber

Raman Fiber	Maximum PbSe-QD/Raman NF	Maximum Raman only	Maximum PbSe-QD only
TrueWave	5.7 dB	10.3 dB	3.0 dB
SMF	4.8 dB	9.8 dB	3.0 dB
LEAF	5.0 dB	9.9 dB	3.0 dB
Corning NZDSF	6.3 dB	10.4 dB	3.0 dB
Corning DSF	6.0 dB	10.4 dB	3.0 dB
ALLWAVE	4.6 dB	9.9 dB	3.0 dB

Table 4. A comparison between PbSe-QD/Raman, EDFA/Raman, and EDFA

Amplifier	Maximum NF
PbSe-QD/Raman	6.3 dB
EDFA/Raman [18]	4.5 dB
EDFA [18]	4.5 dB

4. Conclusion

In this report, through numerical simulations, we studied the NF behavior of a proposed PbSe-QD/Raman amplifier for several commercial Raman fibers. We also studied the variation of the NF with the constituent fibers pumping power and length. Through the change of the size and distribution of the QDs and changing the Raman pumping power scheme and wavelengths this hybrid amplifier would have the advantage of being highly tunable [14]. It was found that increasing the length of the Raman fiber increases the NF for all wavelengths, however, the rate of increase itself slows down with increasing signal wavelength. The increase is highest at the channel with minimum signal wavelength where NF increases from 3 dB for the PbSe QD fiber only amplifier to around 5 dB or 6 dB depending on the type of commercial Raman fiber being considered.

However, the NF figure remains almost constant around 3.2 dB for signal wavelengths of more than 1600 nm. Similar behavior is observed when the pumping power for the Raman amplifier is varied, where for the lowest wavelength channel, the NF increases from around 3.0 dB to a maximum of 6.0 dB for Corning DSF, 5.5 dB for SMF, and less than 6.0 dB for the rest. Increasing the length of the PbSe QD fiber by 10 cm decreases the NF by 3 dB and increasing by 20 cm decreases the NF by around 6 dB and remains almost constant around 3.5 dB after the intersection at a certain wavelength depending on the type of Raman fiber. Similar behavior is observed for the Raman pumping power of the PbSe QD, where increasing the pumping power by 150 mW decreases the NF by 6.0 dB and remains constant for higher pumping power. It is also seen that the NF values are less than those of Raman-only amplifier and are greater than those of EDFA and EDFA/Raman amplifiers.

References

- [1] A. H. Beshr, M. H. Aly, Alexandria Eng. J. **59**(6), 4329 (2020).
- [2] M. A. Iqbal, P. Harper, W. Forsysiak, OSA Technical Digest (online) (Optical Society of America, 2018), paper NpTh1H.2. <https://doi.org/10.1364/NP.2018.NpTh1H.2>
- [3] A. A. Almukhtar et al., Optik **182**, 194 (2019).
- [4] C. Kumar, R. Goyal, J. Opt. Commun. **40**(3), 167 (2019).
- [5] A. Kaur, M. S. Bhamrah, A. Atieh, Opt. Fiber Technol. **52**, 101971 (2019).
- [6] A. Kaur, M. S. Bhamrah, A. Atieh, Lecture Notes in Electrical Engineering **601**, 294 (2020).
- [7] O. Mahran, Opt. Mater. **52**, 100 (2016).
- [8] O. Mahran, Opt. Commun. **353**, 158 (2015).
- [9] C. Cheng, H. Zhang, Opt. Commun. **277**(2), 372 (2007).
- [10] C. Cheng, J. Light. Technol. **26**(11), 1404 (2008).
- [11] C. Cheng, N. Hu, X. Cheng, Opt. Commun. **382**, 470 (2017).
- [12] C. Cheng, F. Wang, X. Cheng, Opt. Laser Technol. **122**, 105812 (2020).
- [13] C. B. Murray, S. Sun, W. Gaschler, H. Doyle, T. A. Betley, C. R. Kagan, IBM J. Res. Dev. **45**(1), 47 (2001).
- [14] H. Du et al., Nano Lett. **2**(11), 1321 (2002).
- [15] Y. Shang et al., Opt. Fiber Technol. **51**, 59 (2019).
- [16] F. Pang et al., Opt. Express **18**(13), 14024 (2010).
- [17] A. V. T. Cartaxo, L. de C. Calmon, M. E. V. Segatto, M. J. Pontes, M. R. N. Ribeiro, S. P. N. Cani, J. Light Technol. **27**(7), 944 (2009).
- [18] O. Mahran, A. Elsamahy, M. Aly, M. Abd, S. Arabia, Optoelectron. Adv. Mat. **9**(5-6), 575 (2015).

*Corresponding author: hassan.yossry_PG@alexu.edu.eg